

Original article

Phase equilibrium calculations in shale gas reservoirs

Tao Zhang, Yiteng Li, Shuyu Sun[✉]**Physical Science and Engineering Division, King Abdullah University of Science and Technology, Thuwal 23955-6900, Saudi Arabia***Keywords:**Phase equilibrium
flash calculation
shale gas
capillary effect
confinement**Cited as:**Zhang, T., Li, Y., Sun, S. Phase equilibrium calculations in shale gas reservoirs. *Capillarity*, 2019, 2(1): 8-16, doi: 10.26804/capi.2019.01.02.**Abstract:**

Compositional multiphase flow in subsurface porous media is becoming increasingly attractive due to issues related with enhanced oil recovery, CO₂ sequestration and the urgent need for development in unconventional oil/gas reservoirs. One key effort to construct the mathematical model governing the compositional flow is to determine the phase compositions of the fluid mixture, and then calculate other related physical properties. In this paper, recent progress on phase equilibrium calculations in unconventional reservoirs has been reviewed and concluded with authors' own analysis, especially focusing on the special mechanisms involved. Phase equilibrium calculation is the main approach to investigate phase behaviors, which could be conducted using different variable specifications, such as the NPT flash and NVT flash. Recently, diffuse interface models, which have been proved to possess a high consistency with thermodynamic laws, have been introduced in the phase equilibrium calculation, incorporating the realistic equation of state (EOS), e.g. Peng-Robinson EOS. In the NVT flash, the Helmholtz free energy is minimized instead of the Gibbs free energy used in NPT flash, and this thermodynamic state function is decomposed into two terms using the convex-concave splitting technique. A semi-implicit numerical scheme is applied to the dynamic model, which ensures the thermodynamic stability and then preserves the fast convergence property. A positive definite coefficient matrix is designed to meet the Onsager reciprocal principle so as to keep the entropy increasing property in the presence of capillary pressure, which is required by the second law of thermodynamics. The robustness of the proposed algorithm is demonstrated by using two numerical examples, one of which has up to seven components. In the complex fluid mixture, special phenomena could be captured from the global minimum of tangent plane distance functions and the phase envelope. It can be found that the boundary between the single-phase and vapor-liquid two phase regions shifts in the presence of capillary pressure, and then the area of each region changes accordingly. Furthermore, the effect of the nanopore size distribution on the phase behavior has been analyzed and a multi-scale scheme is presented based on literature reviews. Fluid properties including swelling factor, criticality, bubble point and volumetrics have been investigated thoroughly by comparing with the bulk fluid flow in a free channel.

1. Introduction

Modeling and simulation of the subsurface fluid flow in porous media have a variety of applications, including reservoir engineering and environmental protection. In petroleum industry, it can be used to simulate various exploitation stages of an oilfield and optimize the development plan for oil recovery maximization. On the other hand, for the increasingly concerned environmental issues (e.g. greenhouse gas emission and pollutant disposal), the simulation of subsurface flow could shed light on the trapping mechanisms of carbon dioxide sequestration or the migration behaviors of underground pollutants (e.g. nuclear waste), which helps to either remarkably reduce the CO₂ emission or controllably dispose the envi-

ronmentally hazardous wastes. The subsurface flow model is formulated based on varieties of conservation laws, including mass conservation, momentum conservation and energy conservation. One key effort to grab these conservation properties is to accurately determine the phase composition; that is, to find out whether the fluid mixture splits into multiple phases or remains in one phase at any given condition. Afterwards, essential physical properties, including density and viscosity, can be calculated thoroughly. Especially, capillary effect, which is often ignored in conventional reservoir simulation, needs to be considered in shale and tight formations, as the nanopores yield a large capillary pressure and confinement effect. It is one of flow mechanisms for the immiscible multiphase flow



*Corresponding author.

E-mail address: tao.zhang.1@kaust.edu.sa (T. Zhang); yiteng.li@kaust.edu.sa (Y. Li); shuyu.sun@kaust.edu.sa (S. Sun).

2652-3310 © The Author(s) 2019.

Received February 12, 2019; revised February 27, 2019; accepted March 3, 2019; available online March 10, 2019.

especially in the formations with strong wettability preference. Surface tension is the main cause of capillary, and it is greatly affected by the phase behaviors and properties of the subsurface fluids. In summary, phase equilibrium calculation is the premise of accurate modeling and simulation of multiphase flow in subsurface porous media (Chareonsuppanimit et al., 2012; Alharthy et al., 2013; Barbosa et al., 2016).

Currently there are two main types of flash techniques for phase equilibrium calculation in petroleum industry. The conventional and popular NPT flash is to perform the iterative calculations based on equation of states with constant mole compositions (N), pressure (P) and temperature (T). The alternative NVT flash investigates the phase equilibrium under a fixed volume rather than pressure, and it minimizes the Helmholtz free energy instead of the Gibbs free energy. NPT flash calculations are proposed earlier, well developed within the last few decades and now become the most commonly used flash technique in oil and gas reservoir simulation. However, it fails to remain the physical meanings in the solution, as a cubic equation derived from equation of state is often needed to be solved. Alternatively, the NVT flash can handle the phase equilibrium calculations as well, without the pressure known a priori. In NVT flash calculations, solving the constrained minimization problem of total Helmholtz free energy takes the main computation consumption, and this is the main focus of designing efficient algorithms. Successive Substitution Iteration (SSI) method was used to solve NVT flash problems by introducing an appropriately defined thermodynamic variable under a similar solution framework to the conventional NPT-flash calculation. Another popular algorithm is using the Newton's method to solve the local minimization problem in combination of the revised Cholesky factorization of the Hessian matrix. Recently, an energy-stable evolution scheme is proposed for NVT flash calculations using diffuse interface models based on the realistic equation of state. In the pore scale model, partial miscibility and compressibility is considered for the first time, and the rigorous mathematical model is established based on fundamental thermodynamic laws, as well as the realistic equation of state (EOS) (e.g. Peng-Robinson). Compared to molecular simulation, which is also capable to capture the diffusive interface behaviors, this extended NVT flash scheme can save a huge portion of CPU time.

In shale gas reservoirs, phase behaviors of subsurface fluid differ from those in bulk phase due to the confinement effects in nanopores and the distribution of pore size in various scales from micrometers to nanometers. The study on fluid flow in nano-scale porous media has been performed before the popularity of shale gas exploration as this effect can also be found in chemical separation design, pollution control or fuel cells. Arising from the endeavor to enhance the shale gas reservoir exploration and exploitation, phase equilibrium studies focusing on the fluid in nanopores have become the interest of modern academia to understand the underlying mechanisms behind the phase behaviors. It has been found that the confinement effects can be affected by pore size distributions, as well as solid-fluid interface interaction properties. Numerous theoretical and experimental studies have been

reported in this area (Wang and Zhang 2006; Wang et al., 2014; Wu et al., 2015). The solid-fluid interaction between pore walls and inside fluid will react on the kinetics and thermodynamics of the fluid flow in the confining geometry significantly, and the isothermal physisorption has been used as an effective approach for fluid components like nitrogen (Li et al., 2005), argon (Li et al., 2018) and intermediate hydrocarbons (Luo et al., 1995). Deep experimental studies have been performed recently to heavy hydrocarbons in the subsurface reservoir with multi-scale distribution of pore size using an isobaric temperature measurement of phase transition (Chareonsuppanimit et al., 2012; Luo et al., 2015; Luo et al., 2016). A differential scanning calorimetry (also known as DSC) technique is applied in their study and the effect of fluid-solid and fluid-fluid interaction in the complex geometry with confining characteristics. Alongside with the definition of fluid-fluid interface interaction defined in bulk fluid flow in free channels, the fluid-solid interface interaction is defined specially in the confined geometry environment and thereby the thermodynamic system is completed (Luo et al., 2017).

Except for the above experimental studies, molecular simulation is also introduced in this area (Nojabaei et al., 2013; Dong et al., 2016; Luo et al., 2019) together with density functional theory (also known as DFT) (Barbosa et al., 2016) and much more interesting and useful insights have been gathered in these theoretical and numerical studies. The classical Lennard-Jones potential is selected in the grand canonical Monte Carlo (also known as GCMC) simulation and the phase transition mechanisms in the fluid structures inside the confining geometry has been analyzed in (Thommes et al., 2002). Compared to the experimental results, a good correlation can be obtained, and the cause of density jump can be attributed to capillary condensation. The jump between the liquid-like state and the vapor-like state often occurs in the measurement of subsurface shale gas reservoirs and the vapor-like state often consists of a low-density core along with certain surface-absorbed layers. It has also been found that the critical temperature of evaporation and condensation can be reduced compared to bulk fluid flow in free channels, and the absorbed phase layering transitions are proven to be the prior mechanism to the short Lennard-Jones chain molecules capillary condensation (Travalloni et al., 2010). Recently, a multi-square-well potential is proposed in DFT, which successfully demonstrates the multi-layering mechanisms in the absorptions on pore walls especially of nano-scale diameters (Trens et al., 2005).

In this paper, we will review the recent progress in the phase equilibrium calculation, which is the key step in the numerical study of compositional multiphase fluid flow in subsurface reservoirs. Compared to the well-developed NPT flash, a major difference in NVT flash calculations is to minimize the Helmholtz free energy instead of the Gibbs free energy. In addition, capillarity, which has been extensively taken into account for phase equilibria problems in unconventional reservoirs, is also treated well in the proposed algorithm. A novel convex splitting scheme of Helmholtz free energy density is presented, to ensure the thermodynamic stability consistent with the second law of thermodynamics.

Regarding capillarity, the work done by the capillary force and the corresponding evolution equations for moles and volume are formulated carefully under rigorous mathematical derivations, with the generalized Onsager coefficient matrix. Furthermore, the modification of Peng-Robinson type EOS is reviewed and the Peng-Robinson-Confined EOS (also known as PR-C EOS) is introduced. This modified PR-type EOS has been successfully used in phase equilibrium calculations with the direct description of solid–fluid interactions between the pore walls and shale gas production fluids, which shows the consistency with the simulation results of molecular simulation and DFT methods. Recently, it has been pointed out that the single-square-well potential used in the description of the solid–fluid interaction is only effective to cases with single layer of absorbed fluid. As a result, the multi-layered fluid properties cannot be properly understood and described, and the difference between the fluid located on the surface and pore center cannot be distinguished significantly. In order to develop a sophisticated model considering the multi-layering effect and meet the experimental data better, a dual-square-well potential is introduced, and the absorbed fluid will be represented by two molecular layers. Another advantage of the dual-square-well potential system is that only one additional parameter is needed to modify the PR EOS with consideration of confinement energy, which has already been determined in previous literatures.

The remainder of this paper is organized as follows. In Section 2, a general diffuse interphase model is constructed combining the NVT flash framework and the first and second laws of thermodynamics to model the multi-component multiphase fluid flow. In Section 3, an energy stable semi-implicit consistent model is presented to simultaneously solve for the phase equilibrium problem with capillarity and numerical examples are presented to show the robustness and efficiency of the concluded scheme. In Section 4, the multi-layering effect is taken consideration to modify the PR EOS and the optimized thermodynamic system is provided. At the end, we make some conclusions and remarks in Section 5.

2. Diffuse interface modeling

In this section, a general diffuse interface model for multi-component multiphase flow is derived rigorously using the first law of thermodynamics for entropy equation and the second law of thermodynamics for the dynamic model. It can be stated from the first law of thermodynamics that

$$\frac{d(U + E)}{dt} = \frac{dW}{dt} + \frac{dQ}{dt} \quad (1)$$

where U is the internal energy, E is the kinetic energy, Q is the heat transfer into the system and W is the work done by the force. The total entropy S can be consists of two contributions, one is the entropy of the system S_{sys} , and the other one is the entropy of the surroundings S_{surr} . The relation between S_{surr} and Q in a reverse process is given by

$$dS_{surr} = -\frac{dQ}{T} \quad (2)$$

Considering the Gibbs relation $U = F + TS_{sys}$, the entropy equation could be written as

$$\begin{aligned} \frac{dS}{dt} &= \frac{dS_{sys}}{dt} + \frac{dS_{surr}}{dt} \\ &= \frac{dS_{sys}}{dt} - \frac{1}{T} \left[\frac{d(U + E)}{dt} - \frac{dW}{dt} \right] \\ &= -\frac{1}{T} \frac{d(F + E)}{dt} + \frac{1}{T} \frac{dW}{dt} \end{aligned} \quad (3)$$

Applying the Reynolds transport theorem and the Gauss divergence theorem, we deduce that

$$\begin{aligned} \frac{dS}{dt} &= \int_{V(t)} \frac{\partial s}{\partial t} dV + \int_{V(t)} \nabla \bullet (\mathbf{u}s) dV \\ \frac{dF}{dt} &= \int_{V(t)} \frac{\partial f}{\partial t} dV + \int_{V(t)} \nabla \bullet (\mathbf{u}f) dV \end{aligned} \quad (4)$$

A symmetric matrix should exist to meet the Onsager's reciprocal principle, which is defined as $\Psi = (\psi_{i,j})_{i,j=1}^{M+1}$ and the time derivatives of mole and volume will become

$$\begin{aligned} \frac{\partial N_{i,n}}{\partial t} &= \sum_{j=1}^M \psi_{i,j} [\mu_j(\mathbf{n}_w) - \mu_j(\mathbf{n}_n)] + \psi_{i,M+1} (p_n - p_w - p_c) \\ \frac{\partial V_n}{\partial t} &= \sum_{j=1}^M \psi_{M+1,j} [\mu_j(\mathbf{n}_w) - \mu_j(\mathbf{n}_n)] + \psi_{M+1,M+1} (p_n - p_w - p_c) \end{aligned} \quad (5)$$

We denote the nonwetting and wetting phase by n and w respectively. The Onsager coefficient matrix, Ψ should be positive definite to keep the growth of total entropy, which is required by the second law of thermodynamics. One simple way to construct the matrix is to design a diagonal positive definite matrix, with the diagonal entry determined by

$$\psi_{i,i} = \frac{D_i N_i^t}{RT}, i = 1, \dots, M, \psi_{M+1,M+1} = \frac{C_n C_w V^t}{C_w p_n + C_n p_w} \quad (6)$$

and the corresponding mole and volume evolutionary equations can be formulated as

$$\begin{aligned} \frac{\partial N_{i,n}}{\partial t} &= \frac{D_i N_i^t}{RT} [\mu_j(\mathbf{n}_w) - \mu_j(\mathbf{n}_n)] \\ \frac{\partial V_n}{\partial t} &= \frac{C_n C_w V^t}{C_w p_n + C_n p_w} (p_n - p_w - p_c) \end{aligned} \quad (7)$$

Here, p_c denotes the capillary pressure, which will be explained in detail in the next session. The thermodynamic stability property of this scheme is achieved on the basis of the convex-concave splitting technique, which is used to decompose the Helmholtz free energy density as follows

$$\begin{aligned} f(\mathbf{n}) &= f^{\text{convex}}(\mathbf{n}) + f^{\text{concave}}(\mathbf{n}) \\ f^{\text{convex}}(\mathbf{n}) &= (1 + \lambda) f^{\text{ideal}}(\mathbf{n}) + f^{\text{repulsion}}(\mathbf{n}) \\ f^{\text{concave}}(\mathbf{n}) &= f^{\text{attraction}}(\mathbf{n}) - \lambda f^{\text{ideal}}(\mathbf{n}) \end{aligned} \quad (8)$$

and correspondingly the chemical potential can be expressed by computing the derivative of the Helmholtz free energy density with respect to the molar density.

3. Phase equilibrium calculation considering capillarity

To meet the requirement in unconventional reservoir simulation, capillarity should be considered in the phase equilibrium calculations. The effects of capillary pressure on the phase equilibrium calculation and reservoir simulation have been investigated thoroughly in previous literatures, with a history of more than 20 years. In 1992, the vapor/liquid equilibrium (VLE) was simulated in the presence of the capillary pressure and a general cubic equation of state is applied. Afterwards, Peng-Robinson EOS and Soave-Redlich-Kwong EOS were used instead and different algorithms were proposed accordingly. A wide range of temperature and pressure had been investigated, but the molecule-surface interactions were neglected, which claimed that the investigated pore size should be more than 10 nm. However, the confinement effect ignored previously have been discovered to greatly impact the fluid properties. With the increasing interaction between pore walls and fluid molecules, the phase behavior in the confined space was suggested to be characterized by introducing the critical pressure and temperature shifts, which were supposed to play important roles in the accurate predictions of phase composition and behaviors in such small nanopores. Nevertheless, recent studies show the shift of critical properties has no solid theoretical basis and its effectiveness is challenged. Although accurate modeling the confinement effect is still debating, the inaccurate simulation of unconventional reservoirs, either for the estimation of original oil in place or ultimate recovery prediction, has been reported to result from the failure to incorporate the capillary effect.

From Session 2, it can be referred that the deviated phase behaviors are the result of the work done by the capillary force during the phase equilibrium process. As a result, it is crucial to quantitatively model this work for the accurate prediction of the phase compositions and behaviors. The capillary pressure is defined by the difference between the pressure of wetting and non-wetting phase, $p_c = p_n - p_w$. If the work done by capillary force is positive, the interface between the two phases will move toward the non-wetting phase, making its volume compressed; otherwise the interface moves toward the wetting phase, which will cause the swelling of non-wetting phase. The work done by the capillary force within certain unit time is given by

$$\begin{aligned} \frac{dW}{dt} &= -p_n \frac{dV_n}{dt} - p_w \frac{dV_w}{dt} \\ &= -p_n \frac{dV_n}{dt} + p_w \frac{dV_n}{dt} \\ &= -p_c \frac{dV_n}{dt} \end{aligned} \quad (9)$$

assuming the capillary pressure to be constant along the interface. There are different equations to get the capillary

pressure, among which the commonly used one is the Young-Laplace equation

$$p_c = \frac{2\sigma \cos \theta}{r} \quad (10)$$

and the Weinaug-Katz correlation

$$\sigma = \left[\sum_{i=1}^M [P]_i (\mathbf{n}_{i,w} - \mathbf{n}_{i,n}) \right]^4 \quad (11)$$

is applied to calculate the interfacial tension used in Eq. 10.

The convex-concave splitting of the Helmholtz free energy density is an approach to ensure the unconditional stability of numerical schemes incorporating thermodynamic dynamics in discrete formulation, as well as the same splitting approach in chemical potential. According to Eq. 8, the chemical potential $\mu_i(\mathbf{n})$ is supposed to have two components $\mu_i^{\text{convex}}(\mathbf{n})$ and $\mu_i^{\text{concave}}(\mathbf{n})$ as well, and the counterparts of the chemical potential can be written as

$$\begin{aligned} \mu_i^{\text{convex}}(\mathbf{n}) &= \frac{\partial f^{\text{convex}}}{\partial n_i} = (1 + \lambda) \frac{\partial f^{\text{ideal}}}{\partial n_i} + \frac{\partial f^{\text{repulsion}}}{\partial n_i} \\ \mu_i^{\text{concave}}(\mathbf{n}) &= \frac{\partial f^{\text{concave}}}{\partial n_i} = \frac{\partial f^{\text{attraction}}}{\partial n_i} - \lambda \frac{\partial f^{\text{ideal}}}{\partial n_i} \end{aligned} \quad (12)$$

To ensure the unconditional stability, the time marching algorithm should also be treated carefully. A semi-implicit scheme, which could conserve the thermodynamic stability at the same time of easy implementation, is introduced in the algorithm. Namely, the implicit scheme is applied on the convex part of chemical potential and Helmholtz free energy density, and the explicit scheme is applied on the concave parts. In order to solve the proposed evolution equations simultaneously, a generalized Onsager coefficient matrix is introduced in the scheme. The two evolution equations, respectively for mole and volume, are solved as follows

$$\begin{aligned} \frac{N_{i,n}^{k+1} - N_{i,n}^k}{\delta t} &= \sum_{j=1}^M \psi_{i,j} (\mu_{j,w}^{k+1} - \mu_{j,n}^{k+1}) \\ &\quad + \psi_{i,M+1} (p_n^{k+1} - p_w^{k+1} - p_c^{k+1}) \\ \frac{V_n^{k+1} - V_n^k}{\delta t} &= \sum_{j=1}^M \psi_{M+1,j} (\mu_{j,w}^{k+1} - \mu_{j,n}^{k+1}) \\ &\quad + \psi_{M+1,M+1} (p_n^{k+1} - p_w^{k+1} - p_c^{k+1}) \end{aligned} \quad (13)$$

The unconditional stability of the above semi-implicit scheme has been proved in detail in (Alharthy et al., 2013). Regarding the Onsager coefficient matrix Ψ , it can be divided into 4 submatrices, shown as below

$$\Psi = \begin{bmatrix} A & B \\ B^T & C \end{bmatrix} \quad (14)$$

where $A = \frac{\partial(\mu_{i,w} - \mu_{i,n})}{\partial N_{i,n}}$, $B = \frac{\partial(\mu_{i,w} - \mu_{i,n})}{\partial V_n} = \frac{\partial(p_n - p_w)}{\partial N_{i,n}}$, $C = \frac{\partial(p_n - p_w)}{\partial V_n}$.

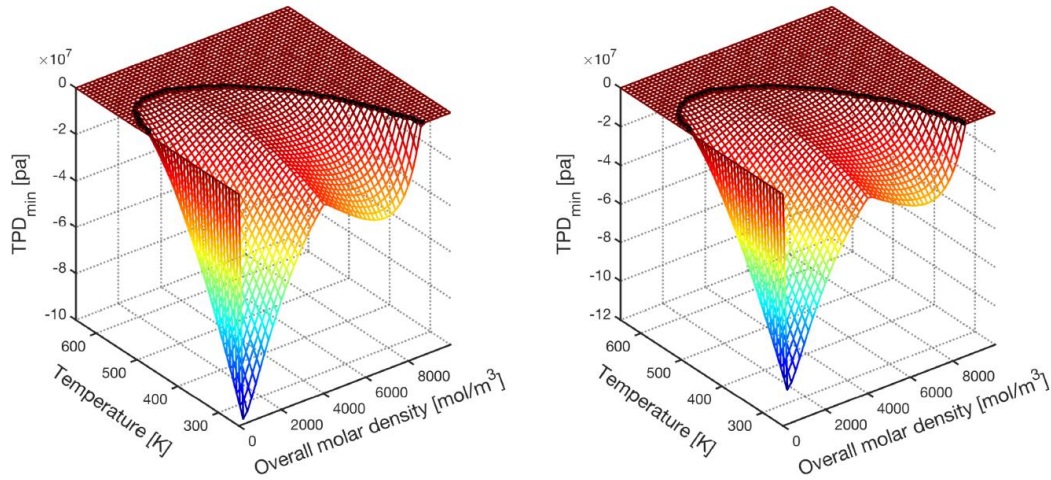


Fig. 1. Global minimum of the TPD function as a function of the overall molar density and temperature for the mixture found in shale gas reservoirs.

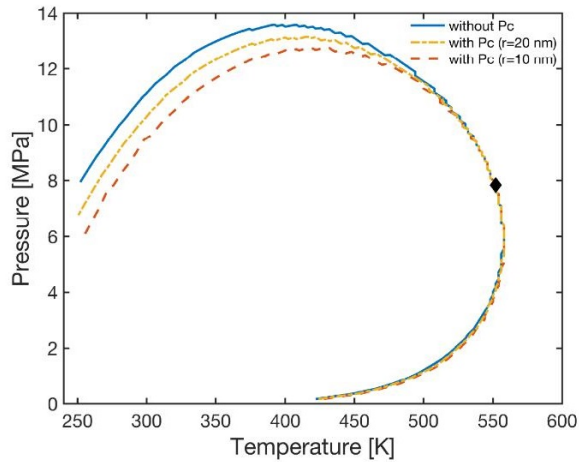


Fig. 2. Phase envelope for the mixture found in shale gas reservoirs with the various consideration of capillary effect.

It is essential to ensure the positive definiteness of the Onsager coefficient matrix; otherwise, a revised Cholesky factorization will be introduced. Generally, $\Psi + E$ should be sufficiently positive and E is added as a diagonal matrix with suitable positive entries. This positive definite property can keep the continuous increasing of entropy in the iterations, which will ensure to reach the local maximum using the Newton-Raphson method.

Based on the algorithm derived above, numerical simulation is performed and the results of the phase equilibrium calculation are presented in Fig. 1. It can be referred from the results that a single two-phase region can be found in the global minimum of the tangent plane distance (TPD) function at the given conditions. The solid black curve represents the boundary between the single-phase region and two-phase region. In the right figure in Fig. 1, the boundary between the vapor-liquid region and single liquid region contracts at large overall concentration, which could be explained by Fig.

2. It is observed that the bulk phase envelope is reshaped by introducing the capillary pressure, which suppressed the bubble point curve remarkably. Meanwhile, a slight outward expansion can be found in the dewpoint curve, which is caused by the insignificant phase boundary expansion at smaller overall concentrations. pressure significantly increases.

Another example is shown in Fig. 3 and Fig. 4 with different components involved. Compared with the last example in (Alharthy et al., 2013) with different overall molar composition, this example exhibits a unique two-phase region as shown in Fig. 3, implying the equilibrium states also rely on the fluid composition. Fig. 4 displays the phase envelopes of all investigated cases. No remarkable deviation from the bulk phase envelope is observed over the entire pressure and temperature windows under the specified pore radii, except a slight change at the tip of the phase envelope where the dew point curve is slightly expanded. This might be attributed to the tiny density differences between two phases under the given overall composition. As the temperature decreases, the bubble point pressure significantly increases.

4. Phase equilibrium calculations considering confinement effect

The multi-layer effect of fluid flow in subsurface porous reservoirs with nano-scale pore size are introduced in the thermodynamic study. Dynamic balance between adsorption and desorption onto the pore wall is analyzed with details. It has been found in the argon fluid that the filling process can be viewed as an adsorption of two layers at first and then four layers occurred in the center. In (Luo et al., 2017), a new methane filling process is proposed and illustrated as shown in Fig. 5. At first, only one single layer of fluid is adsorbed near the surface of the wall in nanotube, as shown in Fig. 5(a) and then another obvious adsorbed molecule layer will be formed, as shown in Fig. 5(b). Phase transitions will be captured as a result of pore filling at the pore center at the same of fully

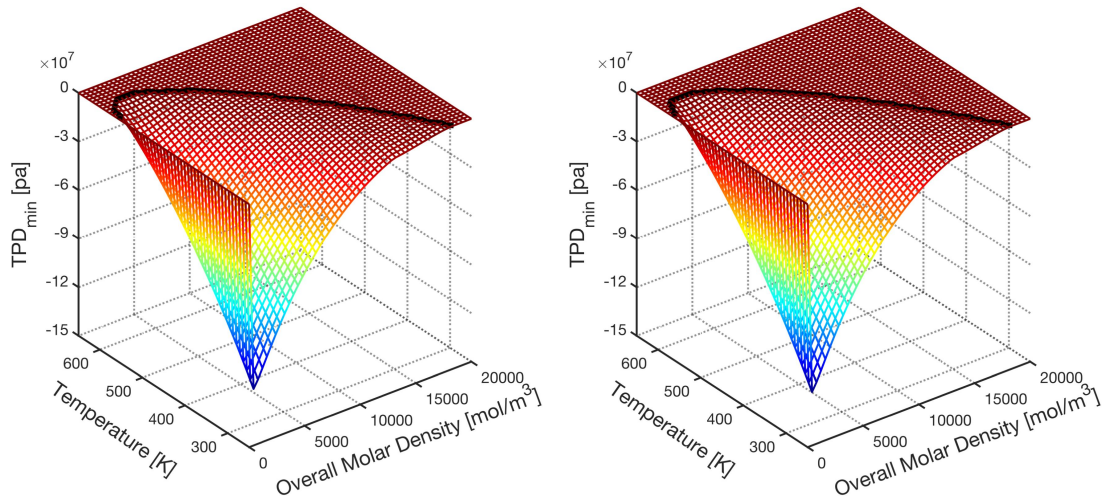


Fig. 3. Global minimum of TPD function of the other mixture found in shale gas reservoirs.

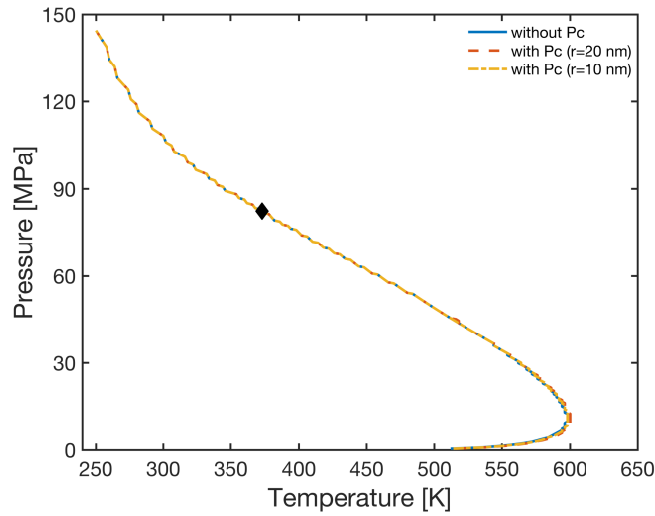


Fig. 4. Phase envelop for the other mixture found in shale gas reservoirs with consideration of various capillary effects.

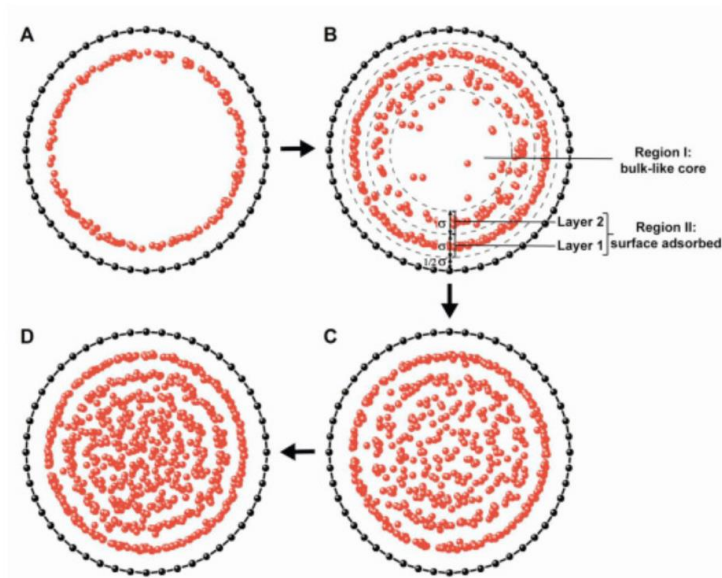


Fig. 5. Snapshots of filling process in nanotube.

filling in the pore, as shown in Fig. 5(c). Furthermore, more molecules will be condensed in the pore center and the nanotube will be densely packed. It can be easily observed from the figure that there are two regions in the pore space. One region is located near the pore center and fluid flow there is similar to bulk fluid in free channel. The other region is located near the pore wall and the solid-fluid interactions cannot be neglected.

Using this definition of multi-layers, the multiple-square-well potential, also known as MSW potential, is effective in describing the layering mechanisms with consideration of the different distance to the wall. A dual-square-well potential is proposed in (Luo et al., 2017) as

$$u_{sf,i}(r) = \begin{cases} \infty, & r < 0.5\sigma_i \\ -\varepsilon_{sf,i}, & 0.5\sigma_i < r < 1.5\sigma_i \\ -\frac{1}{4}\varepsilon_{sf,i}, & 1.5\sigma_i < r < 2.5\sigma_i \\ 0, & r > 2.5\sigma_i \end{cases} \quad (15)$$

The cubic equation of state, represented by Peng-Robinson EOS, is often related with the following equation to model free volume as

$$V_f = V - \sum_{i=1}^M \left(\frac{N_i}{\rho_{\max,i}} \right) \quad (16)$$

The molecular density can be calculated with the following equation with the correlation towards pore size and molecular radius (Quirke and Walton, 1989)

$$\rho_{\max,i}\sigma_i^3 = 1.158 - 0.479 \exp \left[0.621 \left(0.5 - \frac{r_p}{\sigma_i} \right) \right] + 0.595 \exp \left[4.014 \left(0.5 - \frac{r_p}{\sigma_i} \right) \right] \quad (17)$$

For an NVT type flash calculation algorithm, constant particle numbers, temperature and volume are set in the canonical ensemble. A Gaussian-like distribution of the two layers is proposed in (Luo et al., 2017)

$$\begin{aligned} F_{p1} &= F_{pr1} + (1 - F_{pr1})mn \\ m &= \left[1 - \exp \left(-\frac{\beta_0}{T} \right) \right] \\ n &= \left[1 - \exp \left(-\beta_1 \left(\frac{\rho_{\max}}{\rho} - 1 \right)^\gamma \right) \right] \end{aligned} \quad (18)$$

$$\begin{aligned} F_{p2} &= F_{pr2} + (1 - F_{pr2})mn \\ m &= \left[1 - \exp \left(-\frac{\beta_0}{T} \right) \right] \\ n &= \left[1 - \exp \left(-\beta_2 \left(\frac{\rho_{\max}}{\rho} - 1 \right)^\gamma \right) \right] \end{aligned} \quad (19)$$

Data fitting with simulated results of distributions are needed as the fluid-solid interaction between fluid and pore wall and pore size may vary in different cases. Simulation results based on the above scheme has shown that less molecules

will be attracted in the surface layer with if weaker force field is involved and the rising temperature will result in the higher thermal motion in the pore and thereby enhance the random distribution of the fluid molecules, which are both easy to understand and consistent with previous literatures (Zhong et al., 2014).

The modified volume equation of core fluid can be written as

$$V_{co} = V(1 - \bar{F}_{pr2}) \quad (20)$$

and the correlation between surface-absorbed layer fraction \bar{F}_{pr2} and the above distribution F_{p2} can be represented by

$$\bar{F}_{pr2} = \sum_{i=1}^M x_i F_{pr2,i} \quad (21)$$

The Helmholtz free energy in the system can be calculated as

$$\begin{aligned} A &= \sum_{i=1}^M n_i (\mu_{0,i} - RT) + \sum_{rgn=co,sf} (m - n) \\ &- \sum_{i=1}^M \frac{3}{4} N_{av} n_i \varepsilon_{sf,i} [F_{pr1,i} + (1 - F_{pr1,i})p] \end{aligned} \quad (22)$$

$$- \sum_{i=1}^M \frac{1}{4} N_{av} n_i \varepsilon_{sf,i} [F_{pr2,i} + (1 - F_{pr2,i})q]$$

$$m = \sum_{i=1}^M n_{rgn,i} RT \ln \left(\frac{N_{av} x_{rgn,i} \lambda_i^3}{v_{rgn} - b_{p,rgn}} \right)$$

$$n = \left(\frac{\sqrt{2} n_{rgn} a_{p,rgn}}{b_{p,rgn}} \right) \ln \left(\frac{v_{rgn} + (1 + \sqrt{2})b_{p,rgn}}{v_{rgn} + (1 - \sqrt{2})b_{p,rgn}} \right)$$

$$p = \left[1 - \frac{T}{\beta_{0,i}} \left(1 - \exp \left(-\frac{\beta_{0,i}}{T} \right) \right) \right] [1 - \exp(-\beta_{1,i}(\theta - 1)^\gamma)]$$

$$q = \left[1 - \frac{T}{\beta_{0,i}} \left(1 - \exp \left(-\frac{\beta_{0,i}}{T} \right) \right) \right] [1 - \exp(-\beta_{2,i}(\theta - 1)^\gamma)]$$

5. Conclusion and remarks

In this paper, recent progresses on phase equilibrium calculations of subsurface fluids have been reviewed and analyzed with our own understandings. Instead of using the conventional NPT flash, an alternative flash formulation at constant moles, volume and temperature is discussed, which can be used to handle the phase equilibria problems in which the pressure is not known a priori. In the proposed NVT flash calculation, a dynamic model is constructed based on diffuse interface models incorporating realistic EOS, e.g. Peng-Robinson EOS. In order to construct an unconditionally stable numerical algorithm, the total Helmholtz free energy is split by the convex-concave splitting technique, and a semi-implicit time marching scheme is introduced into the dynamic model. For the simulation of phase equilibria in unconventional reservoirs, capillary pressure is taken into considerations, so as

to construct a confined phase equilibrium numerical scheme. The evolution equation of mole and volume are presented to show the dynamic process to the equilibrium state from any initial condition. The proposed algorithm is tested by two numerical examples. The deviated phase behavior in the presence of capillary pressure can be explained reasonably. The phase envelope will be reshaped by capillary effect and the critical point has no change. The bubble point pressure is suppressed in the presence of the capillary pressure, leading to the contraction of the phase boundary between the vapor-liquid region and single liquid region. On the other hand, the phase boundary will expand towards the single vapor region caused by the dew point curve expansion. To extend our study, the confinement and complex pore size distributions will be considered in our further work to simulate more realistic phase equilibrium behaviors in porous media. Furthermore, adsorption is another important factor to determine the phase equilibria in unconventional reservoirs. Thus, the dynamic sorption should be taken into account in the optimization of the diffuse interface-based models. In addition, a pore-size-distribution effect is modeled to modify the Peng-Robinson EOS system to describe the specific phase behaviors of fluid flow in shale gas reservoirs. The Dual-square-well potential function is presented to model the separation of core fluid from the force field on the pore wall.

Acknowledgement

The authors thank for the support from the National Natural Science Foundation of China (No. 51874262) and the Research Funding from King Abdullah University of Science and Technology (KAUST) through the grants BAS/1/1351-01-01.

Conflict of interest

The authors declare no competing interest.

Open Access This article is distributed under the terms and conditions of the Creative Commons Attribution (CC BY-NC-ND) license, which permits unrestricted use, distribution, and reproduction in any medium, provided the original work is properly cited.

References

- Alharthy, N.S., Nguyen, T., Teklu, T.W., et al. Multiphase compositional modeling in small-scale pores of unconventional shale reservoirs. Paper SPE 166306 Presented at SPE Annual Technical Conference and Exhibition, New Orleans, Louisiana, USA, 30 September-2 October, 2013.
- Barbosa, G.D., Travalloni, L., Castier, M., et al. Extending an equation of state to confined fluids with basis on molecular simulations. *Chem. Eng. Sci.* 2016, 153: 212-220.
- Chareonsuppanimit, P., Mohammad, S.A., Robinson Jr, R.L., et al. High-pressure adsorption of gases on shales: Measurements and modeling. *Int. J. Coal Geol.* 2012, 95: 34-46.
- Devegowda, D., Sapmanee, K., Civan, F., et al. Phase behavior of gas condensates in shales due to pore proximity effects: Implications for transport, reserves and well productivity. Paper SPE 160099 Presented at SPE Annual Technical Conference and Exhibition, San Antonio, Texas, USA, 8-10 October, 2012.
- Dong, X., Liu, H., Hou, J., et al. Phase equilibria of confined fluids in nanopores of tight and shale rocks considering the effect of capillary pressure and adsorption film. *Ind. Eng. Chem. Res.* 2016, 55(3): 798-811.
- Hartman, R.C., Ambrose, R.J., Akkutlu, I.Y., et al. Shale gas-in-place calculations part II-multicomponent gas adsorption effects. Paper SPE 144097 Presented at North American Unconventional Gas Conference and Exhibition, The Woodlands, Texas, USA, 14-16 June, 2011.
- Islam, A.W., Patzek, T.W., Sun, A.Y. Thermodynamics phase changes of nanopore fluids. *J. Nat. Gas Sci. Eng.* 2015, 25: 134-139.
- Jin, B., Bi, R., Nasrabadi, H. Molecular simulation of the pore size distribution effect on phase behavior of methane confined in nanopores. *Fluid Phase Equilib.* 2017, 452: 94-102.
- Jin, B., Nasrabadi, H. Phase behavior of multi-component hydrocarbon systems in nano-pores using gauge-GCMC molecular simulation. *Fluid Phase Equilib.* 2016, 425: 324-334.
- Jin, B., Nasrabadi, H. Phase behavior in shale organic and inorganic nanopores from molecular simulation. *SPE Reserv. Eval. Eng.* 2018, 21(3): 626-637.
- Jin, Z., Firoozabadi, A. Thermodynamic modeling of phase behavior in shale media. *SPE J.* 2016, 21(1): 190-207.
- King, G.R. Material-balance techniques for coal-seam and devonian shale gas reservoirs with limited water influx. *SPE Reserv. Eval. Eng.* 1993, 8(1): 67-72.
- Li, Y., Kou, J., Sun, S. Thermodynamically stable two-phase equilibrium calculation of hydrocarbon mixtures with capillary pressure. *Ind. Eng. Chem. Res.* 2018, 57(50): 17276-17288.
- Li, Z., Cao, D., Wu, J. Layering, condensation, and evaporation of short chains in narrow slit pores. *J. Chem. Phys.* 2005, 122(22): 224701.
- Lu, X.C., Li, F.C., Watson, A.T. Adsorption studies of atural gas storage in Devonian shales. *SPE Form. Eval.* 1995, 10(2): 109-113.
- Luo, S., Jin, B., Lutkenhaus, J.L., et al. A novel pore-size-dependent equation of state for modeling fluid phase behavior in nanopores. *Fluid Phase Equilib.* 2019, 498: 72-85.
- Luo, S., Lutkenhaus, J.L., Nasrabadi, H. Experimental study of confinement effect on hydrocarbon phase behavior in nano-scale porous media using differential scanning calorimetry. Paper SPE 175095 Presented at SPE Annual Technical Conference and Exhibition. Society of Petroleum Engineers, Houston, Texas, USA, 28-30 September, 2015.
- Luo, S., Lutkenhaus, J.L., Nasrabadi, H. Confinement-induced supercriticality and phase equilibria of hydrocarbons in nanopores. *Langmuir* 2016, 32(44): 11506-11513.

- Luo, S., Lutkenhaus, J.L., Nasrabadi, H. Multi-scale fluid phase behavior simulation in shale reservoirs by a pore-size-dependent equation of state. Paper SPE 187422 Presented at SPE Annual Technical Conference and Exhibition, San Antonio, Texas, USA, 9-11 October, 2017.
- Nojabaei, B., Johns, R.T., Chu, L. Effect of capillary pressure on phase behavior in tight rocks and shales. *SPE Reserv. Eval. Eng.* 2013, 16(3): 281-289.
- Tan, S.P., Piri, M. Equation-of-state modeling of confined-fluid phase equilibria in nanopores. *Fluid Phase Equilib.* 2015, 393: 48-63.
- Thommes, M., Köhn, R., Fröba, M. Sorption and pore condensation behavior of pure fluids in mesoporous MCM-48 silica, MCM-41 silica, SBA-15 silica and controlled-pore glass at temperatures above and below the bulk triple point. *Appl. Surf. Sci.* 2002, 196(1-4): 239-249.
- Travalloni, L., Castier, M., Tavares, F.W., et al. Thermodynamic modeling of confined fluids using an extension of the generalized van der Waals theory. *Chem. Eng. Sci.* 2010, 65(10): 3088-3099.
- Trens, P., Tanchoux, N., Papineschi, P.M., et al. Confinement effects in MCM-41-type materials: Comparison of the energetics of n-hexane and 1-hexene adsorption. *Microporous Mesoporous Mat.* 2005, 86(1-3): 354-363.
- Walton, J.P.R.B., Quirke, N.P.R.B. Capillary condensation: a molecular simulation study. *Mol. Simulat.* 1989, 2(4-6): 361-391.
- Wang, L., Parsa, E., Gao, Y., et al. Experimental study and modeling of the effect of nanoconfinement on hydrocarbon phase behavior in unconventional reservoirs. Paper SPE 169581 Presented at SPE Western North American and Rocky Mountain Joint Meeting, Denver, Colorado, 17-18 April, 2014.
- Wu, K., Li, X., Wang, C. Model for surface diffusion of adsorbed gas in nanopores of shale gas reservoirs. *Ind. Eng. Chem. Res.* 2015, 54(12): 3225-3236.
- Zhang, X., Wang, W. Square-well fluids in confined space with discretely attractive wall-fluid potentials: Critical point shift. *Phys. Rev. E* 2006, 74(6): 062601.
- Zhong, D.L., Li, Z., Lu, Y.Y., et al. Phase equilibrium data of gas hydrates formed from a CO₂+ CH₄ gas mixture in the presence of tetrahydrofuran. *J. Chem. Eng. Data* 2014, 59(12): 4110-4117.
- Zhu, H.Y., Ni, L.A., Lu, G.Q. A pore-size-dependent equation of state for multilayer adsorption in cylindrical mesopores. *Langmuir* 1999, 15(10): 3632-3641.